ELSEVIER

Contents lists available at ScienceDirect

Advances in Sample Preparation

journal homepage: www.elsevier.com/locate/sampre



Ionic liquid-grafted aminosilica-graphene oxide sorbent for efficient microextraction by packed sorbent of multiclass pesticides in wine

Alessandra Timóteo Cardoso ^{a,b}, Gloria Domínguez-Rodríguez ^b, Alejandro Cifuentes ^{b,*}, Fernando Mauro Lanças ^{a,*}

ARTICLE INFO

Keywords: Multiclass pesticides Wine samples Microextraction by packed sorbent Graphene Oxide Ionic Liquid Direct anion-exchange Liquid Chromatography-Tandem Mass Spectrometry

ABSTRACT

Monitoring pesticide residues in wine is essential for ensuring food safety, as these compounds and their metabolites can persist in the final product and pose potential health risks. This study reports the development of a hybrid sorbent based on graphene oxide anchored to aminosilica particles (GO@Si), functionalized with ionic liquids (ILs) via direct anion-exchange. Among the tested combinations, GO@Si-[VHIm]*PF6* exhibited the best extraction performance due to its multiple interaction mechanisms with analytes. This sorbent was integrated into a microextraction by packed sorbent (MEPS) system for the extraction of six multiclass pesticides from wine, followed by high-performance liquid chromatography-tandem mass spectrometry (HPLC-MS/MS) analysis. After optimizing extraction conditions using univariate and multivariate approaches, the method demonstrated excellent linearity ($r^2 \ge 0.9958$), satisfactory precision (RSDs < 15 %), and recoveries ranging from 49 % to 112 %. Limits of quantification were from 0.030 to 0.130 ng mL $^{-1}$, with negligible matrix effects in white, red, and rosé wines. The method also presented notable green advantages, including device reusability (up to six cycles) and low solvent consumption (0.7 mL per extraction). Sustainability assessments using AGREEprep and BAGI yielded favourable scores (0.52 and 57.5, respectively). This pilot study provides a promising and environmentally conscious analytical approach for multiclass pesticide monitoring in wines, with potential for further development into routine analysis.

1. Introduction

Wine production is a well-established sector in Europe, especially in Italy, France, and Spain [1], holding both economic and cultural significance [2]. However, large-scale viticulture often requires pesticides to prevent significant crop losses [3], which raises concerns about residual contamination in the final product despite post-harvest processing [4]. These contaminants may also disrupt fermentation by affecting the yeast microbiome, altering the polyphenolic composition and sensory characteristics of the wine [5]. In this sense, cumulative pesticide exposure through contaminated food and beverages poses significant risks to human health, including acute and chronic diseases and even poisoning deaths [6].

Given these risks, monitoring emerging pesticide residues in wine is therefore essential. For example, atrazine – a triazine herbicide banned in the European Union (EU) for its persistence and toxicity – has been repeatedly detected in vineyard water sources, [3,7,8]. Similarly,

although carbamates degrade quickly, their toxic metabolites can accumulate in food and water, while their misuse has been reported in Spanish wines [9,10]. In this context, carbendazim, though prohibited, remains widely used in grape cultivation and has been found in red wines from the Canary Islands and the Iberian Peninsula [10]. While the EU defines maximum residue limits (MRLs) for grapes, but not for wine, residues are generally expected to remain below 10 % of the grape MRL [8]. Therefore, analytical methods must offer high sensitivity, with limits of detection (LOD) and quantification (LOQ) below the regulated levels. Thus, an appropriate sample preparation step is essential to ensure that the method can detect trace amounts of pesticides by effectively removing interferents such as polyphenols and sugars, thus enabling reliable quantification.

Techniques such as Quick, easy, cheap, efficient, rugged, and safe extraction method (QuEChERS) and solid-phase extraction (SPE) have been widely applied for pesticide extraction and clean-up in wine samples [9,11]. Additionally, miniaturized techniques have gained

E-mail addresses: a.cifuentes@csic.es (A. Cifuentes), flancas@iqsc.usp.br (F.M. Lanças).

^a Laboratory of Chromatography, São Carlos Institute of Chemistry, Universidade de São Paulo 13566-590 São Carlos, Brazil

^b Laboratory of Foodomics, Institute of Food Science Research, CIAL, CSIC, Nicolás Cabrera 9, Madrid 28049, Spain

^{*} Corresponding authors.

prominence for similar purposes in other complex beverage matrices, offering advantages such as lower solvent consumption, reduced environmental impact, and comparable analytical performance [12,13].

Among these, microextraction by packed sorbent (MEPS) stands out as a promising alternative. MEPS uses a small amount of sorbent (≤ 10 mg) packed in a syringe-like device and requires minimal sample and solvent volumes (in the microliter range). The device can also be reused for multiple extraction cycles, making it efficient and sustainable. However, its performance, as with other sorbent-based methods, depends directly on the selectivity of interactions between the analytes and the sorbent phase [13,14]. In recent years, graphene oxide (GO) anchored onto aminosilica particles (Si) has emerged as an effective sorbent due to its high surface area, π - π interaction capacity, and oxygenated functional groups, which favor the adsorption of structurally diverse pesticides in complex matrices. The aminosilica support not only provides mechanical stability but also prevents aggregation of GO sheets and solvent leakage under pressure, making it compatible with packed sorbent techniques [15–17].

Furthermore, functionalization of GO@Si with materials containing specific functional groups, such as ionic liquids (ILs), could enhance sorbent selectivity. ILs offer tunable interactions with both polar and nonpolar analytes, expanding the range of sorption mechanisms. This tunability arises from the modular combination of cations and anions to tailor ILs with desired physicochemical properties [18]. A widely adopted strategy to modify ILs is direct anion exchange, which enables changing the anion without requiring harsh reaction conditions or specialized equipment [19,20]. This approach allows the straightforward preparation of ILs with diverse functionalities for fine-tuning sorbent performance.

Building on these previous findings, the present work investigates the surface functionalization of GO@Si with imidazolium-based ionic liquids. It introduces structural variations in the ions with distinct physicochemical features to improve sorbent selectivity and demonstrates their application in the extraction of selected pesticides from wine samples. Initially, GO@Si was modified with a hydrophilic ionic liquid (1-vinyl-3-hexylimidazolium bromide), followed by replacement of the bromide ion with four different anions - hexafluorophosphate (PFe $^-$), naphthalene sulfonate (NS $^-$), dodecyl sulfate (DS $^-$), and octane sulfonate (OS $^-$) - via direct anion exchange, generating a set of tailored sorbents.

The resulting sorbents were evaluated for their performance in the extraction of carbamates, triazines, and carbendazim using MEPS. The sorbent exhibiting the highest adsorption capacity for the selected pesticides was thoroughly characterized to confirm its structure, and the extraction method was optimized by investigating the main variables influencing its performance. Method validation followed the guidelines established by SANTE of the EU for pesticide analysis in food matrices. As a proof of concept, the developed method was successfully applied to Spanish wine samples. To the best of our knowledge, this is the first report of graphene oxide anchored on aminosilica and functionalized with tailored ionic liquids being applied in a miniaturized extraction technique for pesticide analysis in wine.

2. Materials and methods

2.1. Materials

Analytical standards of carbendazim (CBZ), thiodicarb (TDC), carbofuran (CBF), carbaryl (CBR), atrazine (ATR), and terbuthylazine were purchased from Sigma-Aldrich (St. Louis, MO, USA). Individual pesticide stock solutions (1 mg mL $^{-1}$) were prepared in methanol and stored at $-4\,^{\circ}$ C. Working standard solutions were prepared weekly by serial dilution in ultrapure water (UHP):acetonitrile (97:3, v/v) for sample fortification.

For synthesis, the following reagents were obtained from Sigma-Aldrich: carbodiimide hydrochloride (EDC), N-hydroxysuccinimide

(NHS, 97 %), amino-functionalized silica gel spherical particles (40–70 μ m), 1-vinylimidazole, 1-bromohexane, 3-mercaptopropyltriethoxyane (MPTES), dimethyl sulfoxide (DMSO), 2,2'-azobis(2-methylpropionitrile) (AIBN, 0.2 M), and anhydrous toluene. For anion exchange, ammonium hexafluorophosphate (NH₄PF₆), sodium naphthalene sulfonate (NaNS), sodium dodecyl sulfate (SDS), and sodium octane sulfonate (NaOS) were also acquired from Sigma-Aldrich.

HPLC-grade solvents included acetonitrile (ACN) and methanol (MeOH) from Panreac Química (Barcelona, Spain), as well as ethanol (EtOH), acetic acid (HAc), and ethyl acetate (EtOAc) from VWR Chemicals (Leuven, Belgium) and formic acid (FA) from Fisher Scientific (Hampton, NH, USA). Ultra-pure water was obtained from a Milli-Q A10 system (Millipore, Massachusetts, USA).

For MEPS extraction, 1 mL polypropylene syringes (HSW Henke-Ject®, without needle) were purchased from Henke Sass Wolf (Tuttlingen, Germany). DSC-18 and Strata-X SPE phases were obtained from Alltech (Deerfield, IL, USA), and the Amino (NH₂) phase was acquired from JT Baker (Phillipsburg, USA).

2.2. Instrumental and conditions

The GO@Si sorbent was dried using a LIOTOP L202 freeze dryer (Liobras, São Carlos, Brazil). Products from subsequent synthesis steps were dried in a Shimadzu CTO-20A HPLC column oven (Kyoto, Japan). The synthesized 1-vinyl-3-hexylimidazolium bromide ([VHIm]⁺Br⁻) ionic liquid was dried using a Thermo Scientific SPD 120 SpeedVac concentrator (Waltham, MA, USA) (see Section 2.3-2.5).

Physicochemical characterization of the sorbents was performed using multiple analytical techniques: scanning electron microscopy with energy-dispersive X-ray spectroscopy (SEM-EDX) analysis was conducted using a JSM 7200F microscope from JEOL (Tokyo, Japan) operating at 5 kV acceleration voltage and magnifications of 2000 x, 3000 \times , 5000 \times and 10,000 \times to examine morphology and elemental composition; Fourier transform infrared spectroscopy (FTIR) spectra were acquired in the 600-4000 cm⁻¹ range using a Bruker Tensor 27 spectrometer (Massachusetts, USA) to identify functional groups; Thermal stability was assessed by thermogravimetric analysis (TGA) on a Discovery 55 instrument from TA Instruments (New Castle, DE, USA) with a heating rate of 10 $^{\circ}$ C min⁻¹ under nitrogen atmosphere (25–800 °C, 50 mL min⁻¹ flow) followed by oxidative conditions (800–1000 °C, air) and surface area and porosity measurements were obtained through nitrogen adsorption at $-195.8\,^{\circ}\text{C}$ using a Micromeritics ASAP 2020 Plus system (Norcross, GA, USA), with data analyzed by the Brunauer-Emmett-Teller (BET) method.

The evaluation of sorbent materials, time required for anion exchange, and MEPS disposable optimization was performed using a Waters M-Class UPLC system (Milford, MA, USA) comprising a micro binary solvent manager, micro sample manager, and Xevo TQ-S Micro mass spectrometer. Chromatographic separation was achieved on an Acquity UPLC M-Class HSS T3 C18 column (300 μ m imes 150 mm, 1.8 μ m) maintained at 30 °C, with a 1 µL injection volume. The mobile phase consisted of water and ACN (both containing 0.1 % formic acid) delivered at 6 μL/min under the gradient conditions specified in Table S1. Mass spectrometric detection was conducted in positive electrospray ionization (ESI+) mode with the following parameters: capillary voltage 2.5 kV, desolvation gas (N2) flow 800 L/h, desolvation temperature 350 °C, and multiple reaction monitoring (MRM) acquisition. The quantification and identification transitions for each pesticide are detailed in Table S2, with data processing performed using MassLynx v4.2 software from Waters Laboratory Informatics.

For method optimization, figures of merit assessment, and real sample analysis, an Accela HPLC system from Thermo Fisher Scientific (Waltham, MA, USA), coupled to a TSQ Quantum Access triple-quadrupole mass spectrometer with an ESI source, was employed. The system included an autosampler, column temperature controller, and quaternary pump. Separations were carried out on a Phenomenex

Table 1Optimized MRM transitions for pesticide analysis.

Analyte	Precursor ion $[M + H] + (m/z)$	Transition (m/z)	Collision energy (eV)	Tube lens offset (V)	Retention time (min)
Carbendazim	192	160.03ª	19	92.60	5.4
		132.10^{b}	33		
Thiodicarb	355	88.20 ^a	14	76.74	9.6
		73.25 ^b	55		
Carbofuran	222	165.07 ^a	11	86.35	10.0
		123.12^{b}	22		
Carbaryl	202	145.09 ^a	11	79.09	10.6
		117^{b}	30		
Atrazine	216	174.01 ^a	19	76.04	11.0
		104.13 ^b	30		
Terbuthylazine	230	174.01 ^a	18	81.84	13.6
		96.25 ^b	29		

^a Quantification transition.

Gemini NX-C18 column (3 µm, 150 mm \times 2 mm) at 40 °C, with a 10 µL injection volume and the same mobile phase composition at 200 µL/min. The gradient program initiated at 3 % B (0–1 min), increased to 40 % B (5 min), then to 50 % B (9 min), and finally to 80 % B (15 min), followed by re-equilibration to 3 % B (16–21 min). MS detection optimized in ESI+ mode utilized a spray voltage of 4500 V, desolvation gas flow of 35 L/h (N₂), and capillary temperature of 215 °C, with MRM acquisition monitoring two transitions per analyte (Table 1). Data analysis was conducted using <code>Xcalibur</code> v2.0 software from Thermo Electron Corporation.

2.3. Syntesis of GO@Si

The GO particles were synthesized from graphite powder via a modified Hummers' method, following a procedure previously established by our research group [21,22]. For GO anchoring onto Si particles, an aqueous amidation reaction was employed [16]. Briefly, 40 mg of GO was dispersed in 80 mL of ultrapure water in a 250 mL flask and sonicated for 1 h. Subsequently, 0.750 mL of an aqueous solution containing 10 mmol $\rm L^{-1}$ EDC and 5 mmol $\rm L^{-1}$ NHS (pre-cooled) was added at room temperature. The mixture was stirred for 30 min, followed by the addition of 1 g of Si particles, and the reaction was maintained at 25 °C for 4 h. The resulting light brown suspension was centrifuged (5000 rpm, 5 min), and the precipitate was washed three times alternately with MeOH and UHP water (six washes total). Finally, the product was lyophilized overnight.

2.4. GO@Si surface modification with thiol groups (GO@Si-SH)

The surface of GO@Si was functionalized with MPTES to enable covalent grafting of IL monomers onto the adsorbent structure via thiol (–SH) groups. For this purpose, 15 mL of anhydrous toluene and 1 mL of MPTES (excess) were added to 1 g of pre-synthesized GO@Si in a 50 mL two-neck round-bottom flask. The reaction was carried out at 110 °C for 24 h under reflux in an inert $N_{\rm 2}$ atmosphere. After that, the flask was cooled to room temperature, and the product was purified via sequential washing with toluene, ethanol (\times 2), UHP water, and methanol. Then, the material was dried in a temperature-controlled oven at 65 °C for 12 h.

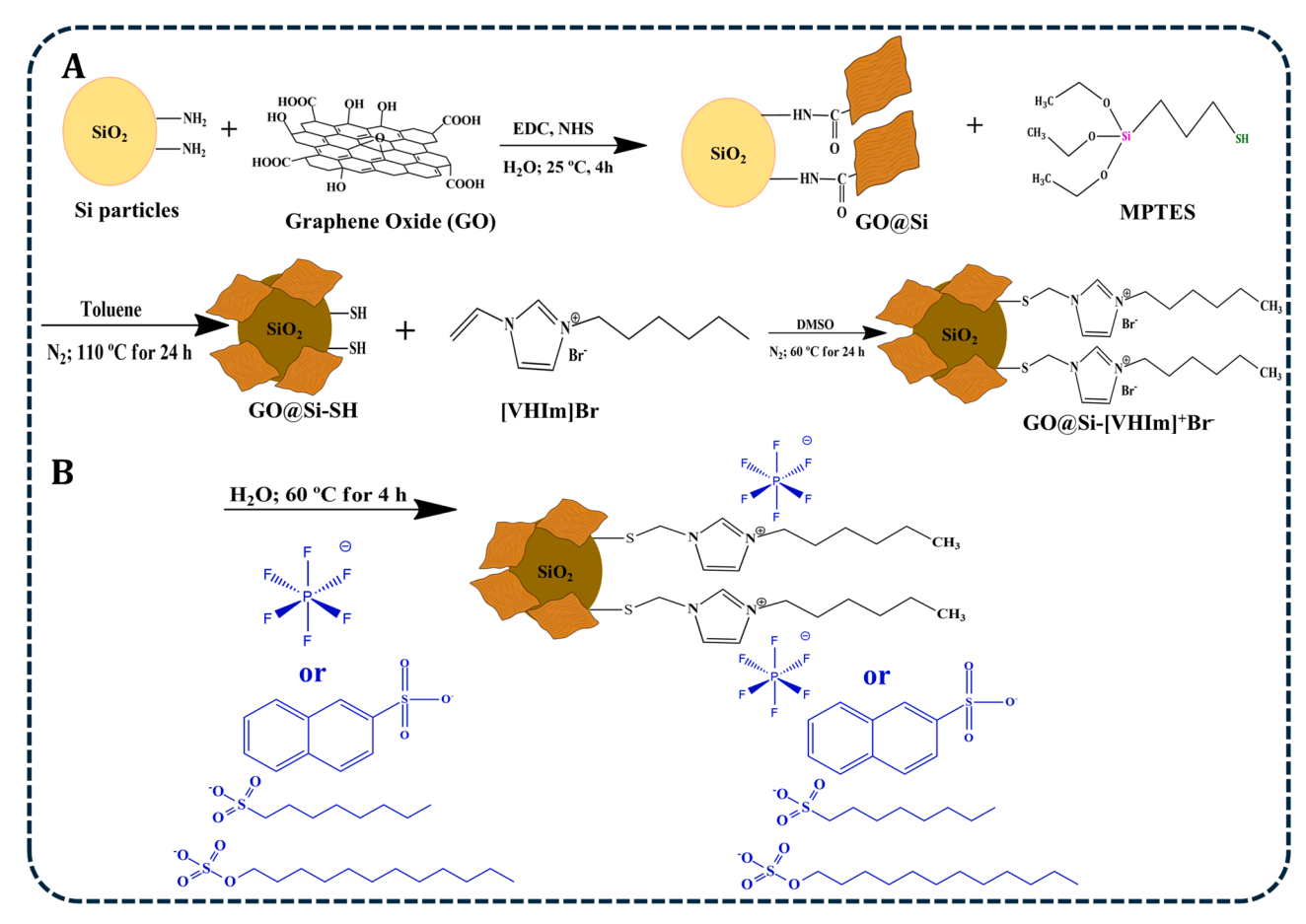


Fig. 1. Reaction scheme for (A) synthesis of ionic liquid-grafted aminosilica-graphene oxide and (B) subsequent anion exchange process.

^b Confirmation transition.

2.5. Anchoring of [VHIm]⁺Br⁻ onto GO@SI-SH surfaces followed by insitu anion exchange

The synthesis of [VHIm] $^+$ Br from 1-vinylimidazole and 1-bromohexane was previously optimized, characterized, and reported by our research group [23]. Subsequently, 2 g of GO@Si-SH and 2 g of [VHIm] $^+$ Br were added to a 50 mL two-neck round-bottom flask containing 40 mL of DMSO and 0.1 g of AIBN (a radical initiator). The reaction was carried out under reflux at 60 °C for 24 h under a N₂ atmosphere. Then, the product was washed sequentially with 15 mL portions of DMSO, ethanol, and methanol, then dried under the same conditions as the previous step, and GO@Si- [VHIm] $^+$ Br was obtained.

For the in-situ anion exchange (Fig. 1B), 1 g of GO@Si-[VHIm] $^+$ Br was mixed with 1 g of NH₄PF₆, NaNS, SDS, or NaOS in 10 mL of UHP water in a 50 mL round-bottom flask. The mixture was sonicated for 30 min to ensure complete dissolution. Subsequently, the reaction was carried out under reflux at 60 °C for 4 h. After cooling, the product was washed repeatedly with UHP water and dried at 60 °C for 12 h in an oven. The complete reaction scheme for all synthetic steps is presented in Fig. 1.

2.6. Extraction capacity assessment and time required for anion exchange optimization

The performance of each prepared sorbent was evaluated using a packed syringe (1 mL) containing approximately 3 mg of each extraction phase immobilized between two polypropylene frits (**Fig. S1A**), as previously reported by Fumes and Lanças [16] and Maciel et al [17]. A standard solution containing six pesticides (100 ng mL $^{-1}$) was prepared in UHP water. The extraction procedure followed these preliminary conditions with draw/eject cycles: (1) conditioning with 5 cycles of 500 μ L water: ACN (97:3, v/v); (2) loading with 10 cycles of 500 μ L standard solution; (3) drying with 4 cycles of 1 mL air aspiration; (4) washing with 4 cycles of 500 μ L UHP water; (5) 10 cycles of desorption with 100 μ L of ACN:MeOH (50:50, v/v); and (6) regeneration with 5 cycles (draw/eject) of 500 μ L ACN to prevent carryover.

The final extract was thoroughly dried under vacuum using a SpeedVac and reconstituted in the original desorption volume with the initial mobile phase composition of the chromatographic gradient. This procedure was systematically applied to all extracts throughout the study. An aliquot of 0.5 μ L was then injected into the UPLC-MS/MS system. All experiments were performed in triplicate. After selecting the most selective extraction sorbent, the anion exchange reaction time (4–24 h) was optimized based on pesticide sorption performance using the same procedures described above.

2.7. Optimization of the MEPS method

After selecting the optimal synthesized sorbent, we evaluated the MEPS disposable configuration, sorbent amount, and desorption solvent using a univariate approach. Two MEPS configurations were compared, each employing 3 mg of the developed sorbent: (1) a standard 1 mL polypropylene syringe fitted with two polypropylene filters [24] and (2) a custom mini-repackable cartridge, as described in our previous work (Fig. S1A-B) [25]. This in-house developed cartridge features the sorbent packed between the removable needle and gastight syringe from Hamilton (Nevada, USA). For MEPS extraction, sorbent quantities ranging from 3 to 10 mg were assessed, with an optimal amount determined based on performance. Additionally, the study tested five solvent systems: MeOH:HAc (99:1, v/v), ACN:MEOH (50:50, v/v), pure ACN, pure MeOH, and EtOAc. All optimization experiments were performed using pesticide-fortified white wine spiked at a concentration of 100 ng mL⁻¹. Subsequently, a 2⁷⁻³ fractional factorial design with three replicates at the central point was employed to screen the most critical MEPS parameters influencing extraction efficiency. The evaluated factors included sample volume (250–750 μ L), desorption volume

Table 2 Experimental levels of variables used in the 2^{7-3} factorial design.

Factors	Levels					
	Low (-)	Central point (0)	High (+)			
Sample Volume (μL)	250	500	750			
Desorption Volume (µL)	150	200	250			
Sampling Cycles	6	8	10			
Washing Cycles	1	3	4			
Desorption Cycles	6	8	10			
Ionic Strength (%NaCl)	0	2,5	5			
Sample pH	3	6	9			

(150–250 μ L), number of sampling and desorption cycles (6–10), number of washing cycles (1-4), ionic strength (0-5 % NaCl), and sample pH (3–9), adjusted with 0.1 M NaOH for pH 6 and 9, and 0.1 M HCl for pH 3. This design resulted in 19 experimental runs, and the levels used are shown in Table 2. Based on the results from the screening, the most influential variables were further optimized using a Box-Behnken design (BBD) combined with response surface methodology (RSM), focusing on sample pH, ionic strength, and the number of sampling cycles. The BBD comprised 15 runs, including 12 factorial points and 3 replicates at the central point, along with their factors and levels (see Table S3). All experimental designs and statistical analyses were conducted using samples spiked at a concentration of 200 ng mL⁻¹. Data processing and statistical analyses of univariate and multivariate experiments were performed using Statistica software (v. 14.0.1; TIBCO, Palo Alto, CA, USA). For univariate optimizations, extraction efficiencies were compared by one-way analysis of variance (ANOVA) followed by Fisher's least significant difference (LSD) test at $p \le 0.05$.

2.8. Method validation

The figures of merit for six pesticides in white wine samples adhered to the guidelines of SANTE/11,312/2021 [26], as recommended by the EU for pesticide residues in food. The parameters evaluated included LOD, LOQ, linearity, recovery, precision, and matrix effect. LOQ was defined as the lowest fortification level where precision met the acceptability criteria established by the SANTE guideline, with a signal-to-noise (S/N) ratio of 10. Also, LOD was defined as the analyte concentration producing an S/N ratio three times higher than the S/N. Linearity was assessed by the coefficient of determination (r²) across five concentration levels. The range was 2-500 ng mL⁻¹ for carbendazim and 0.5-100 ng mL⁻¹ for the other pesticides. Calibration curves were generated by measuring the relationship between concentration and chromatographic peak areas for each analyte in triplicate. The matrix effect (%ME) for white, red, and rosé wines was determined by comparing the slopes of calibration curves obtained from fortified wine extracts to those prepared in solvent (water: ACN, 97:3 v/v), within the same linearity range. The %ME was calculated using Eq. (1), where the slope ratio is expressed as a percentage and reduced by 1.

$$(ME\%) = \left(\frac{\text{slope of matrix}}{\text{slope of solvent}} - 1\right) x \ 100\% \tag{1}$$

Precision was evaluated as repeatability. Experiments were performed in quintuplicate at three concentration levels: 10, 20, and 50 ng $\rm mL^{-1}$ (low, medium, and high, respectively) for carbendazim, and 5, 10, and 20 ng $\rm mL^{-1}$ for the other pesticides. All tests were conducted under identical conditions on the same day. Results were expressed as the relative standard deviation (%RSD). Recovery (%) was determined at the same concentration levels as precision for all the pesticides. The value was calculated by comparing the peak area of the analyte in the extract after the MEPS procedure to the peak area of the blank extracted sample fortified post-extraction, then multiplying the result by 100.

The batch-to-batch reproducibility of the $GO@Si-[VHIm]^+PF_6^-$ sorbent was evaluated by measuring pesticide %RSD from three different

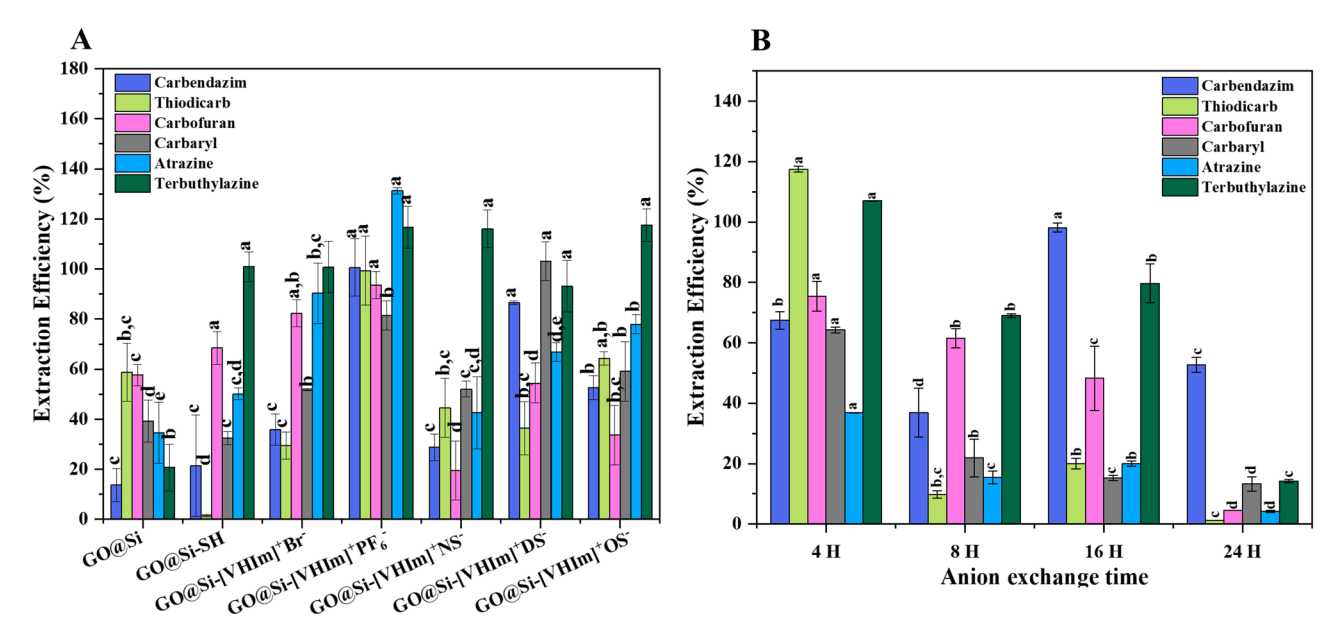


Fig. 2. (A) Comparison of extraction efficiencies for six pesticides using different sorbents. (B) Effect of time required for anion exchange on extraction efficiency during optimization. Superscript letters (a, b, c) indicate statistically significant differences in extraction efficiency ($p \le 0.05$) "a" denotes the highest efficiency, with subsequent letters showing progressively lower performance. Identical letters mean no significant difference.

lots. Each lot was tested in triplicate (n=3) using white wine samples fortified with a pesticide mix at 200 ng mL⁻¹. Concurrently, the reusability rate was assessed by measuring pesticide recovery in five consecutive extractions from wine samples fortified with the same pesticide mix concentration.

2.9. Wine samples

White wine samples used for MEPS extraction optimization and validation were purchased from a supermarket in Madrid, Spain. Before use, chromatographic screening confirmed the absence of the target analytes. For real sample analysis, wines from different regions of Spain – including red and white varieties (**Table S4**) – were obtained from various commercial establishments in Madrid, Spain. All samples were stored at $-5~^{\circ}$ C in the dark until analysis. Before extraction, samples underwent centrifugation (14,000 rpm, 5 min) to remove organic impurities. Following this, red wine was diluted in UHP water (1:5, v/v), rosé wine was diluted (1:2, v/v), while white wine samples were processed without dilution.

3. Results and discussion

3.1. Extraction capacity of adsorbents and time required for anion exchange

The comparison of pesticide extraction performances revealed that the sorbent functionalized with the PF_{6}^{-} anion $GO@Si^{-}$ [VHIm] $^{+}PF_{6}^{-}$ exhibited superior efficiency compared to the other developed materials. This sorbent achieved recoveries ≥ 80 % for most of the investigated pesticides, with statistically significant differences ($p \leq 0.05$) concerning both the unmodified GO@Si and the Br^{-} functionalized version. (Fig. 2A). These findings indicate that direct anion exchange plays a crucial role in enhancing the sorbent's extraction capabilities. Among the tested anions, PF_{6}^{-} conferred the highest extraction efficiency for most of the analytes, except carbaryl. Previous studies have demonstrated that the GO@Si sorbent promotes $\pi^{-}\pi$ interactions between the π -electron system of graphene sheets and the double bonds of aromatic compounds, a common feature among the target pesticides in this study [21,27]. Additionally, the large surface area and mesoporous structure of GO@Si facilitate analyte diffusion and access to active

binding sites. The incorporation of the ionic liquid into this structure introduces additional interaction mechanisms, including electrostatic attractions between its functional groups and ionized analytes. Moreover, hydrogen bonding mediated by highly electronegative atoms in the anion, such as fluorine, enhances interactions in aqueous environments, beyond dipole-dipole interactions involving the imidazolium cation, particularly with polar compounds like thiodicarb and carbendazim [28,29]. Hydrophobic interactions also may occur between the sorbent and less polar compounds, such as triazines, due to the apolar regions present in both the analytes and the sorbent's surface, especially from the organic moieties of the ionic liquid and the graphene-based backbone [30]. Fig. S2 presents a comparison of the extraction efficiencies between the developed GO@Si-[VHIm]+PF6- sorbent and commercial sorbents, including aminosilica, DSC-18, and Strata-X. Overall, the performance of the developed material was comparable to, or even superior to, that of these commercial phases, which can be attributed to its multiple extraction mechanisms.

The time required for anion exchange also influenced the sorbent's performance for the studied analytes, as it directly affects the extent to which the new anion is incorporated into the sorbent's structure. To evaluate this effect, exchange reactions were conducted over periods ranging from 4 to 24 h, and the resulting sorbents were tested for their adsorption efficiency toward the target pesticides. As shown in Fig. 2B, a reaction time of 4 h was statistically significant (p < 0.05) and visually sufficient to ensure efficient extraction for most analytes. Longer exchange times, however, resulted in a decline in extraction performance for most compounds. This effect may be attributed to prolonged stirring during the exchange process, which can damage the surface of the particles, reduce the number of active sites, and consequently decrease the available surface area. Another possibility is that an excess of PF₆anions on the sorbent surface may hinder analyte adsorption by oversaturating the material with functional groups, thus favoring the retention of analytes in the aqueous phase. Moreover, from a practical perspective, performing the anion exchange in just 4 h offers time and energy savings, aligning with the principles of Green Analytical Chemistry.

3.2. Characterization of the best sorbent

Characterization analyses were carried out to confirm the

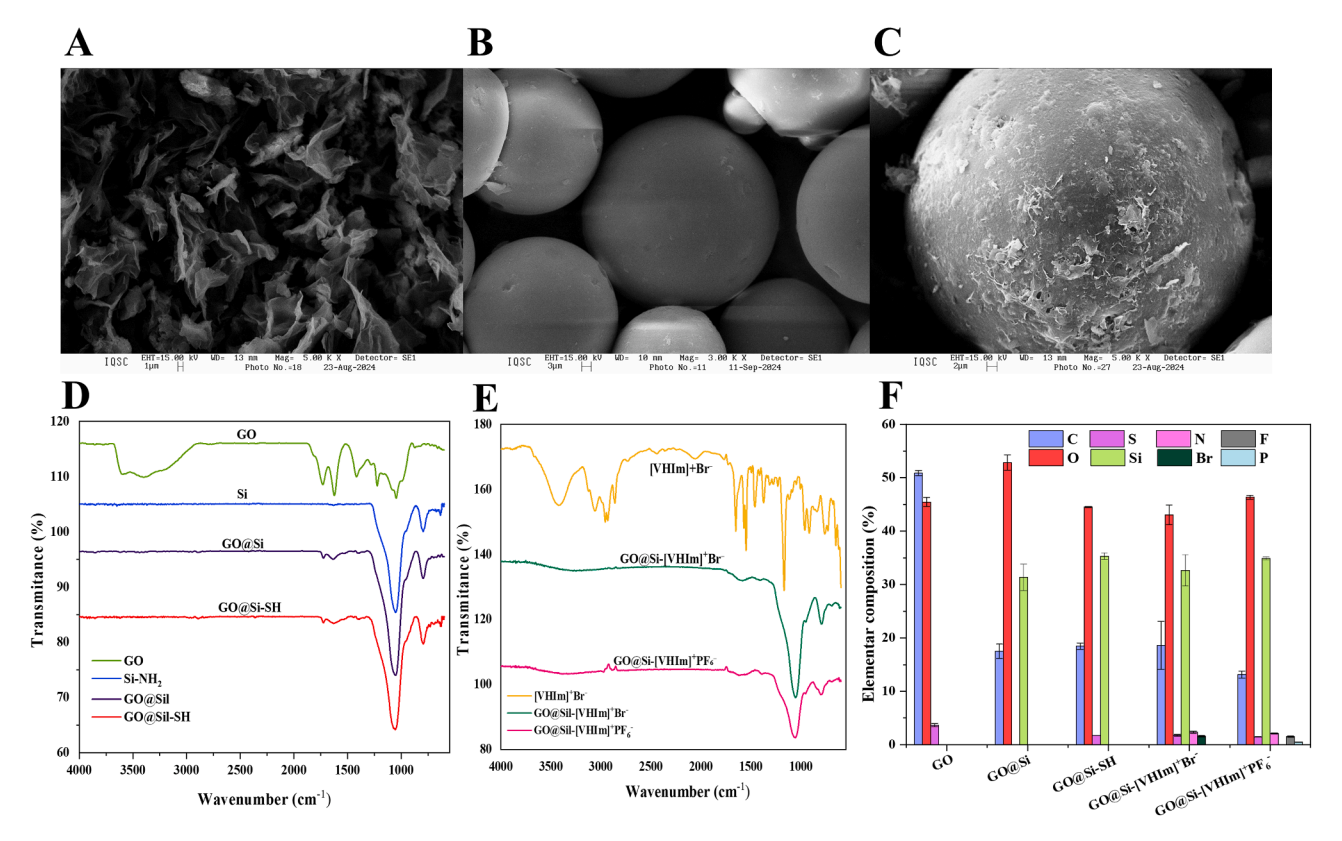


Fig. 3. (A) Scanning electron micrograph of pure GO, (B) pure Si and (C) GO@Si composite; (D-E) FTIR spectra; (F) EDX analysis.

morphological changes, elemental composition, functional groups, and porosity at each stage of the synthesis. In this context, Fig. 3A-C SEM images illustrate the morphological evolution associated with the anchoring of GO nanosheets onto the Si surface.

In Fig. 3A, GO exhibits a continuous and wrinkled sheet-like morphology, characteristic of exfoliated graphene oxide. In contrast, Fig. 3B shows pure Si particles with a smooth and uniform spherical surface, without signs of aggregated structures. However, after the immobilization of GO, Fig. 3C reveals a significant increase in surface roughness, with GO nanosheets observed on the Si surface, indicating successful coating [27].

This morphological change suggests that GO was effectively anchored onto the Si spheres, which not only enhances the adsorptive capacity of the material but also helps prevent sorbent aggregation. As a result, issues such as backpressure or clogging in the MEPS syringe can be minimized during extraction [31]. Furthermore, subsequent functionalization steps with ionic liquids did not significantly alter the overall morphology of the sorbent, as evidenced in Fig. S3, where GO nanosheets remain attached to the Si particles, confirming the structural integrity of the material throughout the synthesis.

In the FTIR spectrum of GO and GO@Si (Fig. 3D), the characteristic functional groups of GO are observed. Notably, the bands at approximately 1049 cm⁻¹ and 1224 cm⁻¹ correspond to the stretching vibrations of C–O and C–OH, respectively. A broad absorption band around 3400 cm⁻¹ is attributed to hydroxyl groups (–OH) present on the two-dimensional surface of GO sheets. Additionally, a peak at 1627 cm⁻¹ corresponds to the C=C stretching vibration in the aromatic rings of graphene, while the band at 1732 cm⁻¹ is associated with C=O stretching, both of which are well-known signatures of oxidized graphene structures [32]. These characteristic bands are also present in the spectra of GO@Si and GO@Si–SH, confirming the successful anchoring of GO sheets onto the Si surface. This is further supported by the FTIR spectrum of pure Si, which lacks these absorption bands. The absence of -OH groups in the GO@Si spectrum also suggests that the reaction was

complete and that Si-binding moieties replaced these functional groups.

Additionally, bands at $1056~\rm cm^{-1}$ and $798~\rm cm^{-1}$ are observed in all Sicontaining materials and correspond to Si-O-Si and Si-O stretching vibrations, respectively, indicating the presence of the Si framework. The FTIR spectra of the ionic liquid-modified sorbents: $GO@Si-[VHIm]^+Br^-$ and $GO@Si-[VHIm]^+PF_6^-$ are shown in Fig. 3E and compared with that of the pure IL $[VHIm]^+Br^-$. A weak but broad band around $1600~\rm cm^{-1}$ corresponds to the C=C stretching of the imidazolium ring, confirming the successful functionalization of the sorbents. In addition, bands in the $2800-3100~\rm cm^{-1}$ region, corresponding to aliphatic C–H stretching, are observed in both functionalized materials and the pure IL, confirming the presence of alkyl chains from the imidazolium cation on the sorbent surface.

Fig. 3F presents the EDX results for each step of sorbent modification. The spectrum of pure GO reveals a predominant composition of carbon (50.9 %) and oxygen (45.5 %), consistent with the structure of oxidized graphene sheets. Upon immobilization onto Si, the carbon content in GO@Si decreases significantly to 17.5 %, which is attributed to the incorporation of the aminosilica matrix. This matrix introduces a substantial amount of silicon (31.3 %) and oxygen (52.8 %), thereby diluting the relative carbon content in the resulting hybrid material. Subsequently, the formation of GO@Si–SH leads to a slight reduction in oxygen content (44.5 %), as some oxygen-containing groups from GO are replaced by thiol functionalities introduced through MPTES. A modest increase in silicon content (35.3 %) is also observed, consistent with the contribution of the silane groups in the functionalization step. No additional elements were detected, supporting the chemical purity of the synthesized materials at each stage.

Finally, the nitrogen adsorption–desorption results are presented in **Table S5**. Compared to pure GO, the anchoring of Si spheres in GO@Si significantly increased the specific surface area of the adsorbent (from 6.75 to 151.28 m 2 g $^{-1}$), which is consistent with previous studies and attributed to the inherently high surface area of Sil particles [33,34]. It is also noteworthy that the type of anion used in the ion-exchange process

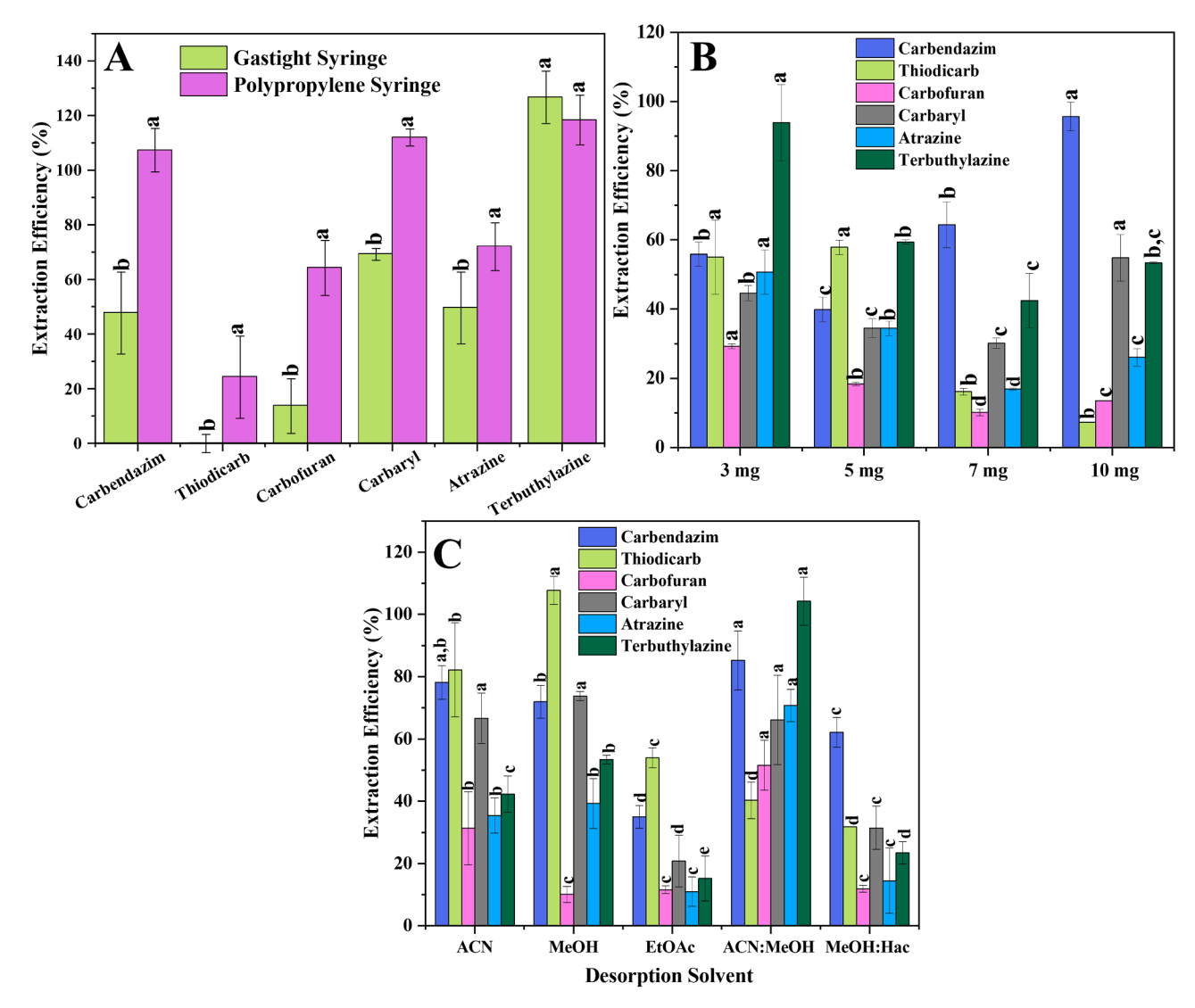


Fig. 4. Impact of MEPS parameters on extraction efficiency: (A) syringe type, (B) sorbent mass, and (C) desorption solvent. Different superscript letters indicate statistically significant differences between conditions ($p \le 0.05$).

influenced the specific surface area, potentially impacting the extraction performance for pesticides. In this context, the PF_6^- anion showed superior performance in pesticide adsorption compared to the other tested anions (NS $^-$, DS $^-$, and OS $^-$). This difference can be mainly attributed to its smaller molecular size, which better preserves the surface area of the GO@Si material, maintaining a greater number of accessible active sites for interaction with pesticide molecules.

In contrast, the larger organic anions tend to partially block the pores and channels of the sorbent structure, significantly reducing accessibility to the adsorption sites. The lower steric hindrance of PF_6^- favors more efficient interactions with pesticides. At the same time, the sulfonate-based anions (NS $^-$, OS $^-$) and DS $^-$ tend to aggregate within the structure, thereby decreasing the available surface area and limiting adsorption efficiency [19].

3.3. Optimization of experimental parameters

3.3.1. MEPS disposable configuration

The MEPS device was evaluated in both standard gastight ($500 \mu L$) and 1 mL polypropylene syringes. While standard MEPS employs gastight syringes, previous studies have explored the polypropylene format due to its greater accessibility [16,24]. Extractions (Fig. 4A) demonstrated that the polypropylene syringe significantly improved

recoveries ($p \leq 0.05$), outperforming the gastight syringe for nearly all pesticides. Furthermore, the packed sorbent bed in polypropylene syringes is more uniform and less prone to backpressure. The inert syringe walls minimize analyte loss. Glass syringes, by contrast, yielded poorer recoveries for most of the polar compounds, likely due to wall adsorption of this polar compound, but offered improved extraction of the more hydrophobic terbuthylazine (log Kow = 3.42). Given its consistent, high recoveries across most analytes and ready availability, the polypropylene syringe was chosen for all subsequent MEPS extractions.

3.3.2. Sorbent amount

The amount of the extractive phase is an essential factor in MEPS, as it influences analyte transfer to the sorbent. Sorbent masses below the optimal level may provide an insufficient number of active sites, resulting in rapid saturation and reduced extraction capacity. In contrast, excessive sorbent can cause back-extraction due to fast equilibrium with the sample matrix [35]. In this work, sorbent amounts ranging from 3 to 10 mg of GO@Si-[VHIm] $^+$ PF $_6^-$ were tested. As shown in Fig. 4B, the 3 mg level yielded significantly higher or comparable extraction efficiencies than higher sorbent amounts for most analytes ($p \le 0.05$), except carbaryl and carbendazim. This observation suggests that, at 3 mg, the available active sites are more effectively accessible, promoting optimal analyte-sorbent interactions and minimizing

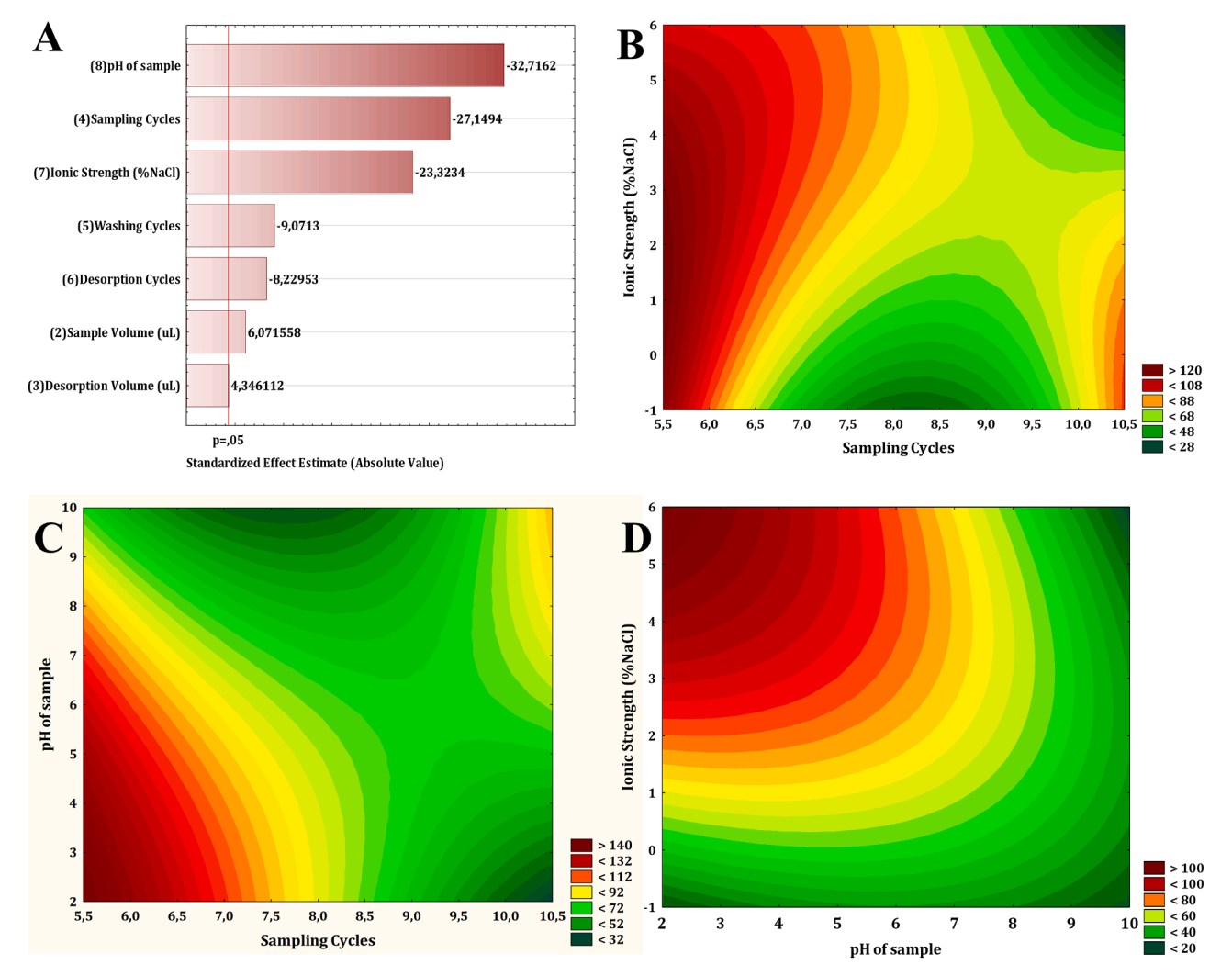


Fig. 5. Visualizing experimental design outcomes. (A) Pareto chart of standardized effects from the 2^{7-3} fractional factorial design. (B–D) Response surface plots from the Box-Behnken design, illustrating interactions: (B) sampling cycles and ionic strength (at fixed sample pH); (C) sampling cycles and sample pH (at fixed ionic strength); and (D) sample pH and ionic strength (at fixed sampling cycles).

potential losses associated with back-extraction. Therefore, it is not solely the absolute number of active sites that determines performance, but rather their effective availability for analyte interaction. Furthermore, using 3 mg also aligns with standard MEPS methods (0.5–10 mg) and supports green chemistry by reducing material use without sacrificing performance [13].

3.3.3. Desorption solvent

The desorption solvent was optimized by testing organic solvents with varying polarity, considering the analytes' polar to moderately polar nature (log Kow 1.33-3.42). Based on the principle of chemical affinity, a 50:50 (v/v) ACN:MeOH mixture provided the best overall performance for the majority of compounds, which was statistically significant ($p \le 0.05$) (see Fig. 4C). This can be attributed to the complementary properties of MeOH (hydrogen bonding) and ACN (dipolar aprotic nature and π - π interactions), resulting in a solvent system with intermediate polarity [36]. For instance, carbaryl showed no significant difference (p > 0.05) with MeOH, ACN, and their mixture due to favorable but distinct interactions. For thiodicarb, the most polar analyte (log Kow = 1.33), methanol was most effective, and the ACN:MeOH mixture yielded the lowest recovery, likely due to less favorable solvation in the mixed system. Considering both efficiency and reproducibility, the ACN:MeOH (50:50, v/v) mixture was selected as the optimal desorption solvent, as it provided balanced recovery across most analytes.

3.3.4. Multivariate optimization

To perform a preliminary evaluation of the most influential factors for MEPS extraction based on reported literature, a $2^{7\text{-}3}$ fractional factorial design was carried out. The factors evaluated at high and low levels, with a center point, included sample and desorption volume, number of sampling, desorption and washing cycles, ionic strength, and sample pH. For this optimization step, recoveries for each analyte were determined using calibration curves constructed by plotting concentration versus analytical response in the range of 10–1000 ng mL $^{-1}$, considering 200 ng mL $^{-1}$ as 100 % recovery.

For data processing, both individual recoveries for each compound and the average recovery of all pesticides combined were considered as response variables. Pareto charts were constructed to assess the significance of each variable. As shown in Fig. 5A, when considering the average recovery of all compounds, all factors—except for desorption volume—were statistically significant. Among them, the number of sampling cycles, sample pH, and ionic strength had the most pronounced influence on recovery, all showing an adverse effect. When analyzing the individual Pareto charts for each analyte (Fig. S4), it is evident that at least one of these three variables appears among the top three most influential factors for each compound. Therefore, these variables were selected for further optimization using a Box-Behnken

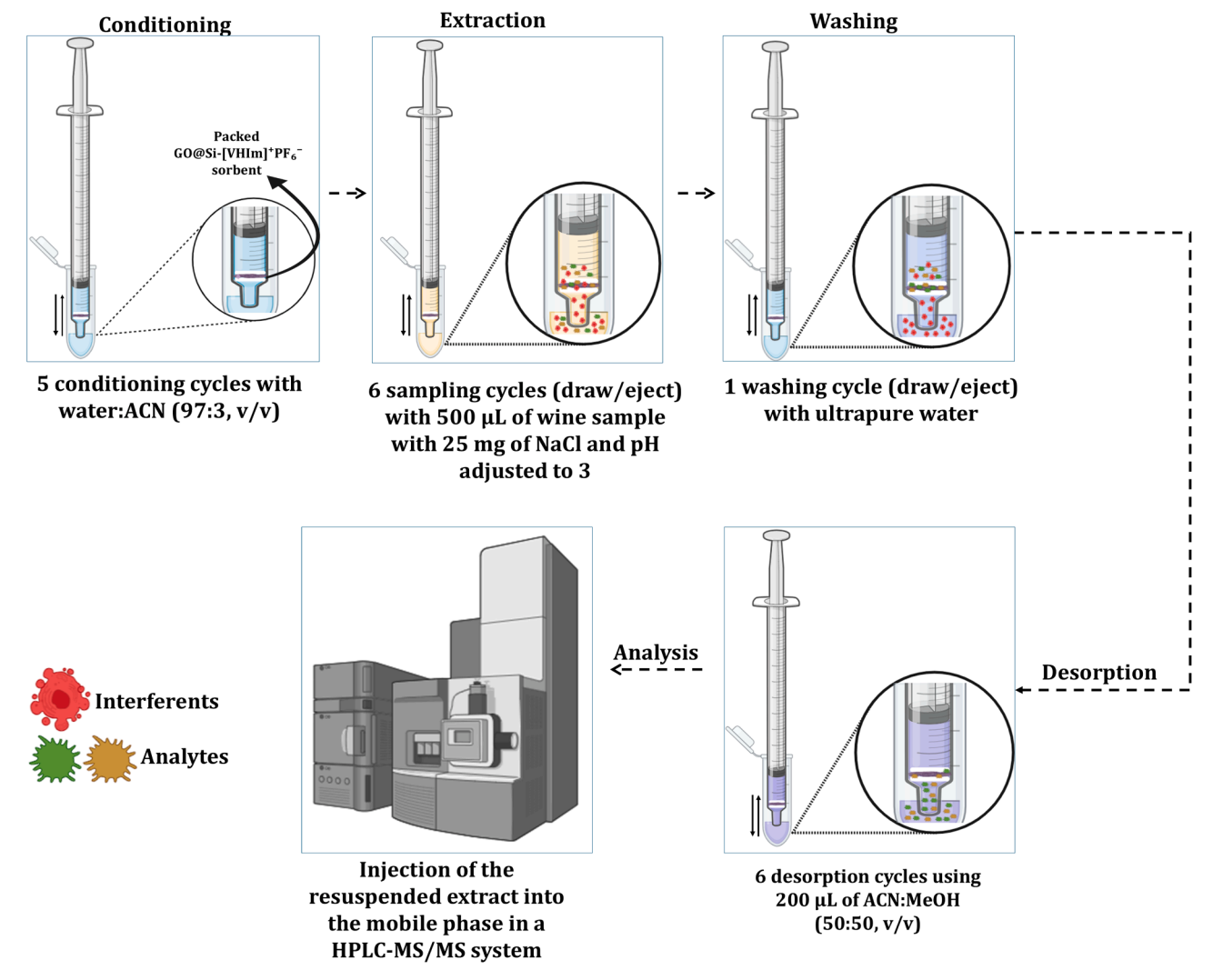


Fig. 6. Optimized MEPS parameters for the extraction of selected pesticides from wine samples. (https://www.biorender.com/).

design, considering a wider range of levels to determine the optimal conditions and enhance extraction efficiency [37].

Other parameters that showed lower influence in the 2^{7-3} factorial design were selected by considering their statistical effects both individually and collectively, as well as insights from previously reported MEPS-based methods. As shown in Fig. 5A, increasing the sample volume resulted in a moderate improvement in overall recoveries. When evaluated individually (Fig. S4), carbendazim, tiodicarb, and carbaryl exhibited a positive effect, while atrazine and terbuthylazine were negatively impacted. Carbofuran showed no significant variation. This behavior may be associated with competition among analytes for the active sites of the sorbent. A higher analyte load may favor the retention of some compounds, while others may undergo back-extraction into the sample matrix, reducing their recovery [38,39]. According to these findings, the intermediate volume of 500 μ L was selected to ensure balanced performance in multiresidue applications.

The washing step is essential to eliminate co-extracted interferences, improve extract clean-up, and reduce matrix effects [13,40]. Due to the high-water solubility of several wine components, including polyphenols, UHP water was selected as the washing solvent [24]. Increasing the number of washing cycles significantly reduced the recovery of most analytes (Fig. S4), likely because their intermediate-to-high polarity favors elution during repeated aqueous washes. As the analytes were determined by HPLC-MS/MS operated in MRM mode, which provides high selectivity, a single washing cycle was chosen to ensure optimal

recovery.

The desorption volume was not significant for the average recovery of all analytes and did not show a substantial effect on carbendazim individually. However, the increase in desorption volume harmed carbofuran, atrazine, and terbuthylazine. Previous studies have shown that lower desorption volumes enhance pre-concentration and improve recovery [24,25]. In this study, for thiodicarb and carbaryl, an increased desorption volume had a positive effect. To achieve a balanced recovery across all compounds and ensure good performance for thiodicarb and carbaryl, the desorption volume was set at 200 μL . Considering the influence of desorption cycles, an increase in draw–eject repetitions led to a negative impact on analyte recoveries (Fig. 5A). When analyzed individually, only thiodicarb showed a significant positive effect; however, this factor had a minor influence compared to others for the same compound. Thus, the lowest level (6 cycles) was selected for subsequent method optimization.

Finally, a Box-Behnken design was carried out to evaluate the optimal conditions for the number of sampling cycles, sample pH, and ionic strength. A total of 15 experiments were performed (**Table S3**), and the results were statistically assessed using ANOVA (**Table S6**). The significance of each factor was evaluated based on the F- and p-values. Factors with p-values below 0.05 were considered statistically significant, indicating a relevant effect on the response variable at a 95 % confidence level. In this study, the number of sampling cycles and sample pH were found to be highly significant, including their linear and

Table 3Analytical Performance of GO@Si-[VHIm]⁺PF₆-MEPS method for multiclass pesticides in wines.

Pesticide ^a MRL for grapes ng mL ⁻¹		Regression Equation	R^2	LODb	LOQ ^c	Level	%RSD ^d	%Recovery $n=5$	Matrix Effect (%)		
	y = ax + b		ng mL ⁻¹	ng mL ⁻¹	ng mL ⁻¹	n = 5		White	Red	Rosé	
CBZ	CBZ 500	y = 29456x + 1E + 06	0.9958	0.012	0.040	10	6.7	105	-8	8	10
						20	9	110			
						50	14	112			
TDC	TDC 10	y = 2786.3x + 13,566	0.9965	0.008	0.030	5	6.6	69	19	-0.3	9
						10	12	53			
						20	10	49			
CBF	CBF 2	y = 17197x + 27,002	0.9964	0.030	0.093	5	14	53	-3	0.7	6
						10	9	65			
						20	11	50			
CBR	CBR 10	y = 19700x + 146,865	0.9992	0.040	0.130	5	10	88	-1	-6	-6
						10	10	98			
						20	13	100			
ATR 50	y = 49091x + 82,288	0.9994	0.011	0.038	5	11	54	-9	-0.5	1	
					10	11	51				
						20	6	67			
TBZ	10	y = 180432x - 193,786	0.9984	0.012	0.042	5	9	76	-2	6.5	-18
						10	6	73			
						20	14	98			

^a CBZ: Carbendazim, TDC: Thiodicarb, CBF: Carbofuran, CBR: Carbaryl, ATR: Atrazine, TBZ: Terbuthylazine;

quadratic effects, as well as some interactions. Ionic strength showed a lower but still significant contribution. The regression model obtained using Statistica software was statistically significant (p=0.000009<0.05), with an R² of 0.9999 and an adjusted R² of 0.9967, confirming its good fit and predictive power. Additionally, the lack-of-fit test was not significant (p=0.083>0.05), indicating no evidence of systematic error. Response surface models were generated to determine the optimal experimental conditions, and the corresponding contour plots are shown in Fig. 5B–C.

As shown in Fig. 5B, the highest response was achieved when sampling cycles were at their lowest level (6 cycles) combined with medium to high ionic strength (2,5–5 % of NaCl). Similarly, Fig. 5C indicates that low to medium sample pH (3–6) interacting with a low sampling cycle (6 cycles) also resulted in high recovery. Finally, Fig. 5D reveals optimal responses when the sample pH is low (3) and the ionic strength is high (5 %).

These observations might be consistent with what one would expect for an MEPS technique. For instance, a low number of sampling cycles (6 cycles) appeared to yield a notably superior extraction performance compared to medium and high levels. This could potentially be due to excessive cycles leading to reverse desorption and sorbent saturation, which might then reduce the sorbents' lifespan. A similar trend was observed with sample pH: higher levels seem to correlate with poorer extraction, whereas samples adjusted to pH 3 generally showed satisfactory recovery values. In complex samples such as wine, excessively high pH levels can lead to the dissociation of phenolic compounds and other matrix components, which may interact with the analytes and hinder their release from the sample matrix retention.

On the other hand, increasing ionic strength with NaCl (at $2.5\,\%$ and $5\,\%$) generally appeared to improve extraction, with minimal difference in recovery between these two higher concentrations. To help pinpoint the optimal conditions for these factors and to validate other parameters, a desirability function (DF) was employed in the analysis of the BBD results (Fig. S5). The established sampling cycles and sample pH aligned well with the response surface profiles. Desirability Function (DF) analysis indicated similar performance between 2.5 % and 5 % NaCl concentrations; however, the 5 % NaCl level was identified as the optimal condition when combined with the other factors. Consequently, optimal parameters for the extraction were determined to be: 6 extraction cycles with 500 μ L of sample (containing 25 mg of NaCl at pH 3), followed by 1 washing cycle, and 6 desorption cycles using 200 μ L of

ACN:MeOH (50/50, v/v). Fig. 6 summarizes the optimized method according to the established steps.

3.4. Analytical performance and reusability of sorbents

Fig. S6 presents the chromatogram of a blank wine sample spiked with six pesticides: carbendazim at 100 ng mL⁻¹ and the other pesticides at 50 ng mL⁻¹, following the MEPS extraction procedure. The analytical performance metrics are summarized in Table 3. The developed method exhibited LODs ranging from 0.08 to 0.30 ng mL⁻¹ and LOQs from 0.030 to 0.130 ng mL⁻¹. These values are lower than the MRLs for each compound, as recommended by SANTE guidelines [26].

The comparison of these metrics considered the MRL equivalents, calculated as 10 % of the MRLs established by the European Commission (EU) for grape wine cultivation (Table 3), as specific regulations for pesticide monitoring in wines are currently unavailable [41]. Method linearity was achieved using a matrix-matched approach. Five concentration levels were evaluated for each analyte, plotting their chromatographic peak areas against concentration. The linearity range was 2–500 ng mL $^{-1}$ for carbendazim and 0.5–100 ng mL $^{-1}$ for the other pesticides. The method demonstrated good linearity, with coefficients of determination $(r^2) \geq 0.9958$ for all compounds.

Recovery and intraday precision were measured at three concentration levels (low, medium, and high) in five replicates. Recovery values, calculated as described in Section 2.8, ranged from 49 % to 112 %. This range is acceptable according to SANTE guidelines, particularly for miniaturized extraction methods like the one in this study, where recoveries between 30 % and 140 % are permitted, provided the method demonstrates adequate precision (%RSD values do not exceed 20 %). Although acceptable according to the guideline used, which also considers the extraction method employed, some pesticides (such as thiodicarb, carbofuran, and atrazine) showed recoveries below 70 %. This outcome may be attributed to factors such as the high complexity of the wine matrix, stronger interactions of these analytes with matrix components compared to the interaction with the developed sorbent, or even to the multiresidue nature of the method, which allows competition among analytes for the active sites and functional groups of the sorbent phase [42].

Nevertheless, even with recoveries below 70 %, precision was the determining factor for considering these results reproducible and suitable for quantification purposes. The precision evaluation further

^b Limit of detection;.

c Limit of quantification:.

d Relative standard deviation.

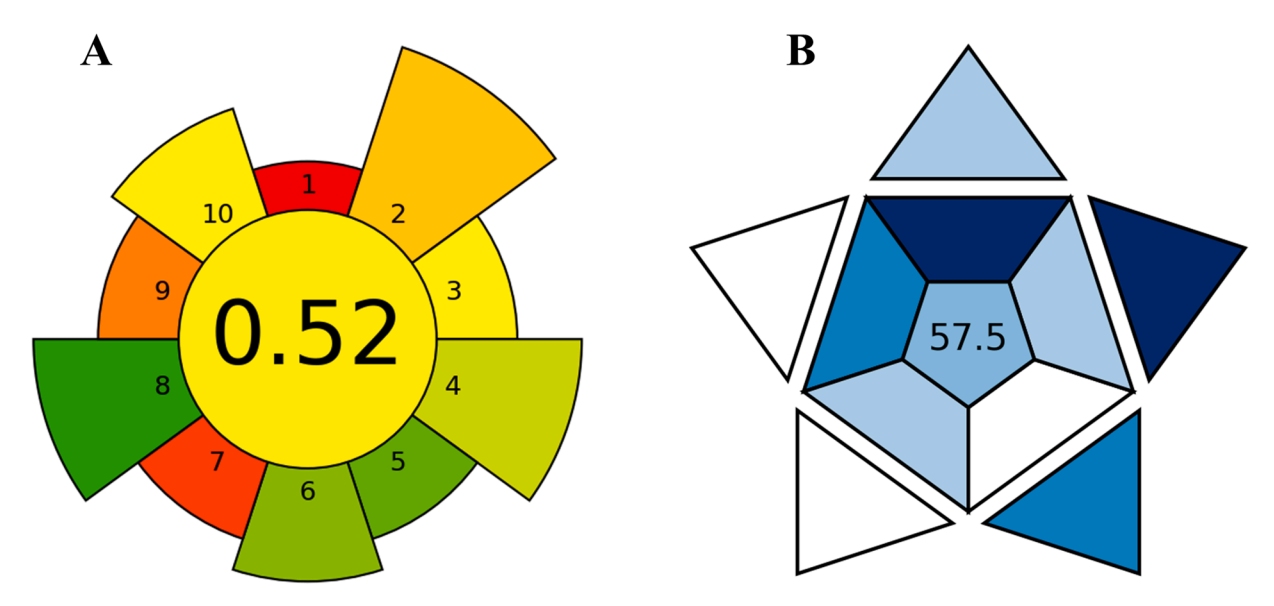


Fig. 7. Greenness and applicability metrics for the developed method. (A) AGREEprep and (B) BAGI pictograms.

supported this, as %RSD values for all pesticides at the three concentration levels (n=5) were consistently below 15 %, thereby meeting guideline criteria. Additionally, as presented in Table 3, the matrix effect (%ME) values for the white wine matrix ranged from -1 % to 19 %. For red wine, the values ranged from -0.3 % to 8 %, and for rosé wine, from -18 % to 10 %. These results indicate that the method significantly reduced matrix effects, with all observed %ME values falling within the acceptable ± 20 % range as per SANTE guidelines. This confirms the method's applicability for the analysis of white, red, and rosé wine samples.

Moreover, the reusability of the extraction device was assessed using white wine samples spiked with a pesticide mix at a concentration of 200 ng mL $^{-1}$. Extractions were performed using the developed GO@Si-[VHIm] $^+PF_6$ -MEPS method. After each extraction, the syringe was regenerated with 5 cycles of 500 μL of ACN to avoid carryover. The extraction efficiency (%) of compounds was calculated as described in Section 3.3.4, serving as the main parameter for evaluating device performance.

Fig. S7 presents the bar graphs for each pesticide over six extractions, revealing that the extraction efficiency remained consistently similar. This indicates that there was no loss in sorbent efficiency after multiple uses. The precision of the consecutive extraction procedures using the same disposable device met the acceptance criteria (all %RSDs below 20 %), with individual values being: 9 % for carbendazim, 10 % for thiodicarb, 12 % for carbofuran, 10 % for carbaryl, 11 % for atrazine, and 6.7 % for terbuthylazine. The batch-to-batch reproducibility of the GO@Si- [VHIm]⁺PF₆ sorbent was evaluated by the method described in Section 2.8. At a concentration of 200 ng mL⁻¹, the relative standard deviations (%RSDs) obtained were 2 % for carbendazim, 2 % for thiodicarb, 10 % for carbofuran, 2 % for carbaryl, 14 % for atrazine, and 9 % for terbuthylazine. This consistency in results confirms the reproducibility of the synthesis.

3.5. Analysis of real samples

As a proof of concept, nine wine samples of different types (white, red, and rosé) from various regions of Spain were analyzed to evaluate the method's applicability. None of the target analytes were detected in the samples, or their concentrations were below the method's LOQ.

3.6. Greenness assessment and comparative method analysis

The main objective of this study was to evaluate the

functionalization of the GO@Si phase with ionic liquids formed from the imidazolium cation (VHIm⁺) and different anion combinations. These ionic liquids were obtained via direct anion exchange, and their sorption properties for multiclass pesticides in complex samples like wine. Despite being a pilot study, the results demonstrated a high adsorptive capacity of the GO@Si- [VHIm]⁺PF₆⁻ phase for the selected pesticides. This efficiency is attributed to favorable interaction mechanisms between the extracting phase and the analytes, which, in turn, increases the method's detectability by mitigating matrix interference effects. Given the promising methodological performance, the method's greenness and applicability metrics were subsequently evaluated using the Analytical Greenness Metric for Sample Preparation (AGREEprep) [43] and Blue Applicability Grade Index (BAGI) [44] tools, respectively.

As illustrated in Fig. 7A, the method achieved a green score of 0.52 by AGREE prep. Its main advantages include employing a relatively low volume of organic solvents (700 μL in total: 200 μL of desorption solvent across all six extraction cycles, and 500 μL of ACN for device regeneration), using only 500 μL of sample, and an extraction time of merely 3 min per sample, allowing for the extraction of 20 samples per hour. Additionally, the energy consumption during the extraction process is relatively low, as it involves only the vacuum drying step, with the capability to process over 40 samples simultaneously. Fig. 7B presents the overall method's applicability score, which includes extraction and analysis, and was evaluated by the BAGI software, indicating a value of 57.5. Although not exceptional, this value is considered acceptable. Key advantages include the quantitative and confirmatory nature of the analysis and the fact that the miniaturized extraction method consumes relatively low sample inputs.

Although direct comparisons with MEPS applied to wine are scarce, the AGREEprep and BAGI scores obtained in this study are comparable or superior to those reported for MEPS procedures developed for other pesticides and contaminants in food matrices. For instance, our group recently applied MEPS with a silica-based sorbent modified with a zwitterionic ionic liquid for the extraction of PAHs in coffee [24]. That method achieved a BAGI score similar to the present work but had a lower AGREEprep score (0.45), mainly due to the use of larger volumes of toxic solvents and samples, which resulted in 4.55 mL of waste. Similarly, a molecularly imprinted polymer (MIP) developed by our group for the extraction of sulfonylurea herbicides in corn [25] yielded an AGREEprep score of 0.49 and a BAGI score of 55.0, reflecting high solvent consumption, the generation of 2.22 mL of waste per extraction, and the analysis of only four analytes from a single class.

Another study investigating MEPS for three pesticides in apple juice

Table 4
Comparison of the developed MEPS method with other extraction techniques for multiclass pesticide determination in wine samples.

Sample preparation ^a	Pretreatment steps	Analytical technique ^b	Total extraction time (min)	Organic waste volume (mL)	Sample volume (mL)	LOQ ^c (ng mL ⁻¹)	Ref.
QuEChERS	7	GC-MS/MS and LC-MS/MS	32	2	1	-	[4]
QuEChERS	9	LC-MS/MS	12	10.5	1	2.60-21.39	[10]
QuEChERS	9	UHPLC-MS	12	11	10	0.01	[9]
SPE	5	LC-MS/MS	_	8	2	0.5-10	[11]
LPME	7	GC-MS	30.17	0.07	12	0.007 - 1.77	[47]
DLLME	4	LC-MS	3	2.0	10	0.0024 - 5.0	[48]
MEPS	5	LC-MS/MS	3	0.7	0.5	0.030- 0.130	This study

^a **LPME:** liquid-phase microextraction; **DLLME:** dispersive liquid-liquid microextraction;.

showed a slightly higher AGREEprep score (0.58) due to the low waste volume (250 µL). However, the sorbent could only be used once, leading to increased waste generation overall. The BAGI score remained similar to that of the present study [40]. In the same field, an earlier study using reduced-graphene-ZnO nanocomposites for the extraction of four carbamate pesticides from fruit juice achieved an AGREEprep score of 0.41 and a BAGI score of 55.0, primarily due to the higher sample volume (5 mL), the generation of 7.25 mL of waste, and a longer extraction time (8 min) [45]. Compared with these methodologies, the present work achieved a significant improvement in sustainability by reducing total waste generation (total volume of sample and organic solvent) to only 1.2 mL and employing a faster extraction step. In addition, the developed GO@Si-[VHIm] +PF6-MEPS procedure allowed the simultaneous extraction of six pesticides from three different classes, increasing its applicability and versatility. Altogether, these features contributed to improving greenness and applicability scores, suggesting that the proposed method can combine efficiency, selectivity, and environmentally responsible performance.

Future improvements to the extraction method may be explored, such as evaluating more classes and compounds, implementing a multisyringe system for simultaneous and automated extraction [46], and pursuing a greener synthesis of the $GO@Si-[VHIm]^+PF_6^-$ extracting phase in terms of the reagents employed. It is worth emphasizing that, although the synthesis of the developed material remains relatively labor-intensive, the overall yield reaches approximately 1 g. Considering that the optimized sorbent amount required for the extraction of a single sample in this study is 3 mg, this yield allows for the preparation of approximately 333 samples, without considering the potential for sorbent reusability.

Table 4 presents a comparison between the developed GO@Si-[VHIm] *PF6-MEPS method and other studies in the literature employing multiclass pesticide extraction in wines. Although this pilot study evaluates fewer compounds than other studies in the table, critical aspects like the number of preparation steps and the method's LOQ range are comparable to well-established methods such as SPE and QuEChERS. The MEPS method stands out for being miniaturized, exhibiting a substantially shorter execution time and low waste generation compared to conventional sample preparation methods. Furthermore, it utilizes simple extraction devices, such as polypropylene syringes, which can be reused multiple times.

4. Conclusion

This paper reports the functionalization of the GO@Si surface with different combinations of imidazolium-based ionic liquids, varying both the cation and anions with distinct physicochemical properties, and, for the first time, its application in the extraction of selected carbamates, triazines, and one benzimidazole from wine samples. This functionalization enhanced the sorption capacity compared to unmodified GO@Si,

with the ionic combination [VHIm] $^+PF_6^-$ showing the best performance among the tested anions. Physicochemical characterization analyses confirmed the successful synthesis of GO@Si and its functionalization with the ionic liquid. A MEPS combined with an HPLC-MS/MS method was then developed, with optimized extraction conditions and satisfactory analytical parameters following the SANTE guidelines for pesticide analysis in food. The method was subsequently applied to the study of selected pesticides in various types of wine samples. In addition, the extraction device is simple, utilizing a polypropylene syringe, only 3 mg of the sorbent, and can be reused up to six times without loss of extraction efficiency. The method may also have potential for the monitoring of other pesticide classes in wine. Improving the simultaneous extraction process may further enhance its practicality, contributing to a greener method suitable for routine analysis.

CRediT authorship contribution statement

Alessandra Timóteo Cardoso: Writing – original draft, Validation, Methodology, Investigation, Formal analysis, Data curation, Conceptualization. Gloria Domínguez-Rodríguez: Validation, Formal analysis, Data curation, Conceptualization. Alejandro Cifuentes: Writing – review & editing, Supervision, Resources, Conceptualization. Fernando Mauro Lanças: Writing – review & editing, Supervision, Resources, Project administration, Funding acquisition, Conceptualization.

Declaration of competing interest

The authors declare no conflict of interest.

Acknowledgments

This study was financed, in part, by the São Paulo Research Foundation (FAPESP), Brasil (Process Numbers: 2024/12325–6; 2023/06258–1 and 2023/07159–7), Conselho Nacional de Desenvolvimento Científico e Tecnológico, (CNPq - Grant 140399/2022–4; 308843/2019–3 and Instituto Nacional de Ciência e Tecnologia de Alimentos - INCT-ALIM Grant 406760/2022–5). Additional support was provided by projects PID2020–113050RB-I00 and PDC2021–120814-I00, funded by MCIN/AEI10.13039/501100011033 and the European Union Next Generation EU/PRTR. This work was also supported in part by the INCGLO0019 project (Bioprospection of local agricultural resources as a pathway to achieve the Sustainable Development Goals). Furthermore, Gloria Domínguez-Rodríguez acknowledges support from the 'Juan de la Cierva' grant JDC2023–052516-I, funded by MCIU/AEI/10.13039/501100011033 and the European Social Fund Plus (FSE+).

Supplementary materials

Supplementary material associated with this article can be found, in

^b GC-MS/MS: gas chromatography-tandem mass spectrometry; UHPLC-MS: Ultra-high performance liquid chromatography-tandem mass spectrometry; GC-MS: gas chromatography-mass spectrometry; HPLC-MS: liquid chromatography-mass spectrometry.

the online version, at doi:10.1016/j.sampre.2025.100217.

Data availability

Data will be made available on request.

References

- J. Carroquino, N. Garcia-Casarejos, P. Gargallo, Classification of Spanish wineries according to their adoption of measures against climate change, J. Clean. Prod. 244 (2020) 118874, https://doi.org/10.1016/j.jclepro.2019.118874.
- [2] L. Casadó-Marín, V. Anzil, Analysis of wine-related cultural consensus in two Spanish wine-producing regions, Int. J. Gastron. Food Sci. 28 (2022) 100536, https://doi.org/10.1016/j.ijgfs.2022.100536.
- [3] E. Herrero-Hernández, M.S. Andrades, A. Álvarez-Martín, E. Pose-Juan, M. S. Rodríguez-Cruz, M.J. Sánchez-Martín, Occurrence of pesticides and some of their degradation products in waters in a Spanish wine region, J. Hydrol. 486 (2013) 234–245, https://doi.org/10.1016/j.jhydrol.2013.01.025.
- [4] P. Alonso González, E.Parga Dans, A.C. Acosta Dacal, M. Zumbado Peña, O. Pérez Luzardo, Differences in the levels of sulphites and pesticide residues in soils and wines and under organic and conventional production methods, J. Food Compos. Anal. 112 (2022) 104714, https://doi.org/10.1016/j.jfca.2022.104714.
- [5] L. Pérez-Mayán, M. Ramil, R. Cela, I. Rodríguez, Determination of pesticide residues in wine by solid-phase extraction on-line combined with liquid chromatography tandem mass spectrometry, J. Food Compos. Anal. 104 (2021) 104184, https://doi.org/10.1016/j.jfca.2021.104184.
- [6] M. Tudi, H. Li, H. Li, L. Wang, J. Lyu, L. Yang, S. Tong, Q.J. Yu, H.D. Ruan, A. Atabila, D.T. Phung, R. Sadler, D. Connell, Exposure routes and health risks associated with pesticide application, Toxics 10 (2022) 10060335, https://doi.org/ 10.3390/toxics10060335.
- [7] D.P. Manjarres-López, M.S. Andrades, S. Sánchez-González, M.S. Rodríguez-Cruz, M.J. Sánchez-Martín, E. Herrero-Hernández, Assessment of pesticide residues in waters and soils of a vineyard region and its temporal evolution, Environ. Pollut. 284 (2021) 117463, https://doi.org/10.1016/j.envpol.2021.117463.
- [8] E. Herrero-Hernández, M.S. Rodríguez-Cruz, E. Pose-Juan, S. Sánchez-González, M. S. Andrades, M.J. Sánchez-Martín, Seasonal distribution of herbicide and insecticide residues in the water resources of the vineyard region of La Rioja (Spain), Sci. Total Environ. 609 (2017) 161–171, https://doi.org/10.1016/j.scitotenv.2017.07.113.
- [9] Á. Santana-Mayor, R. Rodríguez-Ramos, A.V. Herrera-Herrera, J.E. Conde-González, B. Socas-Rodríguez, Food safety assessment of wines commercialised in the Canary Islands by monitoring of pesticide residues from 2017 to 2019, Food Control. 153 (2023) 109957, https://doi.org/10.1016/j.foodcont.2023.109957.
- [10] Á. Santana-Mayor, R. Rodríguez-Ramos, B. Socas-Rodríguez, C. Díaz-Romero, M.Á. Rodríguez-Delgado, Comparison of pesticide residue levels in red wines from Canary Islands, Iberian Peninsula, and Cape Verde, Foods 9 (2020) 9111555, https://doi.org/10.3390/foods9111555.
- [11] V. Fernández-Fernández, M. Ramil, P. Blanco, M.S. Andradres, I. Rodríguez, Pesticides in wines from two major production regions in the North of Spain, J. Food Compos. Anal. 142 (2025) 107525, https://doi.org/10.1016/j. jfca.2025.107525.
- [12] L. Yang, R. Said, M. Abdel-Rehim, Sorbent, device, matrix and application in microextraction by packed sorbent (MEPS): a review, J. Chromatogr. B Analyt. Technol. Biomed. Life Sci. 1043 (2017) 33–43, https://doi.org/10.1016/j. ichromb.2016.10.044.
- [13] A. Firoozichahak, D. Soleymani-ghoozhdi, S. Alizadeh, R. Rahimpoor, Microextraction by packed sorbents (MEPS): fundamental principles and nanomaterial-based adsorbents, TrAC Trends Anal. Chem. 181 (2024) 118043, https://doi.org/10.1016/j.trac.2024.118043.
- [14] D.A. Vargas Medina, A.T. Cardoso, E.V.S. Maciel, F.M. Lanças, Current materials for miniaturized sample preparation: recent advances and future trends, TrAC Trends Anal. Chem. 165 (2023) 117120, https://doi.org/10.1016/j. trac.2023.117120.
- [15] A.T. Cardoso, R.O. Martins, F.M. Lanças, Advances and applications of hybrid graphene-based materials as sorbents for solid phase microextraction techniques, Molecules 29 (2024) 29153661, https://doi.org/10.3390/molecules29153661.
- [16] B.H. Fumes, F.M. Lanças, Use of graphene supported on aminopropyl silica for microextraction of parabens from water samples, J. Chromatogr. A 1487 (2017) 64–71, https://doi.org/10.1016/j.chroma.2017.01.063.
- [17] E. Vasconcelos Soares Maciel, B. Henrique Fumes, A. Lúcia de Toffoli, F. Mauro Lanças, Graphene particles supported on silica as sorbent for residue analysis of tetracyclines in milk employing microextraction by packed sorbent, Electrophoresis 39 (2018) 2047–2055, https://doi.org/10.1002/elps.201800051.
- [18] T.T. Nguyen, T.T.T. Huynh, N.H. Nguyen, T.H. Nguyen, P.H. Tran, Recent advances in the application of ionic liquid-modified silica gel in solid-phase extraction, J. Mol. Liq. 368 (2022) 120623, https://doi.org/10.1016/j.molliq.2022.120623.
- [19] Y. Ding, J. Feng, M. Sun, Y. Feng, X. Xin, M. Sun, Extraction improvement of ionic liquid-functionalized silica by in situ anion-exchange for online solid-phase extraction of estrogens in honey, Food Chem 445 (2024) 138706, https://doi.org/ 10.1016/j.foodchem.2024.138706.
- [20] X. Hou, X. Lu, S. Tang, L. Wang, Y. Guo, Graphene oxide reinforced ionic liquid-functionalized adsorbent for solid-phase extraction of phenolic acids, J. Chromatogr. B Analyt. Technol. Biomed. Life Sci. 1072 (2018) 123–129, https://doi.org/10.1016/j.jchromb.2017.11.013.

- [21] T.C. Oliveira, F.M. Lanças, Determination of selected herbicides in sugarcane-derived foods by graphene-oxide based disposable pipette extraction followed by liquid chromatography-tandem mass spectrometry, J. Chromatogr. A 1687 (2023) 463690, https://doi.org/10.1016/j.chroma.2022.463690.
- [22] L.A. Akamine, D.A. Vargas Medina, F.M. Lanças, Magnetic solid-phase extraction of gingerols in ginger containing products, Talanta 222 (2021) 121683, https://doi. org/10.1016/j.talanta.2020.121683.
- [23] A.T. Cardoso, F.M. Lanças, Graphene oxide functionalized with hydrophilic ionic liquid as stir bar coating: sorptive extraction of selected triazines in grape juice samples, Anal. Chim. Acta 1343 (2025) 343691, https://doi.org/10.1016/j. aca.2025.343691.
- [24] M. Jordan-Sinisterra, D.A. Vargas Medina, F.M. Lanças, Microextraction by packed sorbent of polycyclic aromatic hydrocarbons in brewed coffee samples with a new zwitterionic ionic liquid-modified silica sorbent, J. Food Compos. Anal. 114 (2022) 104832, https://doi.org/10.1016/j.jfca.2022.104832.
- [25] F.N. Andrade, A.J. Santos-Neto, D.A.V. Medina, F.M. Lanças, A molecularly imprinted polymer for microextraction by packed sorbent of sulfonylureas herbicides from corn samples, J. Food Compos. Anal. 121 (2023) 105388, https:// doi.org/10.1016/j.jfca.2023.105388.
- [26] T. Pihlström, A.R. Fernández-Alba, C. Ferrer Amate, M.Erecius Poulsen, B. Hardebusch, M. Anastassiades, Analytical quality control and method validation procedures for pesticide residues analysis in food and feed, Sante (2021), 11312/ 2021, https://www.eurl-pesticides.eu/docs/public/tmplt_article.asp?CntID=727. accessed June 15, 2024.
- [27] E.V.S. Maciel, J.V.B. Borsatto, K. Mejia-Carmona, F.M. Lanças, Application of an inhouse packed octadecylsilica-functionalized graphene oxide column for capillary liquid chromatography analysis of hormones in urine samples, Anal. Chim. Acta 1239 (2023) 340718, https://doi.org/10.1016/j.aca.2022.340718.
- [28] H. Zhang, X. Wu, Y. Yuan, D. Han, F. Qiao, H. Yan, An ionic liquid functionalized graphene adsorbent with multiple adsorption mechanisms for pipette-tip solidphase extraction of auxins in soybean sprouts, Food Chem 265 (2018) 290–297, https://doi.org/10.1016/j.foodchem.2018.05.090.
- [29] L. Dieu Nguyen, N. Hoang Nguyen, M. Hoang Ngoc Do, T. Thai Nguyen, T. Hao Nguyen, C. Thien Gia Hua, P. Hoang Tran, Functionalized ionic liquids as an efficient sorbent for solid-phase extraction of tetracyclines in bovine milk, Microchem. J. 204 (2024) 110999, https://doi.org/10.1016/j.microc.2024.110999.
- [30] K. Mejía-Carmona, F.M. Lanças, Modified graphene-silica as a sorbent for in-tube solid-phase microextraction coupled to liquid chromatography-tandem mass spectrometry. Determination of xanthines in coffee beverages, J. Chromatogr. A 1621 (2020) 461089, https://doi.org/10.1016/j.chroma.2020.461089.
- [31] E.V.S. Maciel, K. Mejía-Carmona, M. Jordan-Sinisterra, L.F. da Silva, D.A. Vargas Medina, F.M. Lanças, The current role of graphene-based nanomaterials in the sample preparation arena, Front. Chem. 8 (2020) 00664, https://doi.org/10.3389/ fchem.2020.00664.
- [32] Y. Yuan, Y. Zhang, M. Wang, J. Cao, H. Yan, Green synthesis of superhydrophilic resin/graphene oxide for efficient analysis of multiple pesticide residues in fruits and vegetables, Food Chem 450 (2024) 139341, https://doi.org/10.1016/j. foodchem.2024.139341.
- [33] X. Hou, S. Liu, P. Zhou, J. Li, X. Liu, L. Wang, Y. Guo, Polymeric ionic liquid modified graphene oxide-grafted silica for solid-phase extraction to analyze the excretion-dynamics of flavonoids in urine by Box-Behnken statistical design, J. Chromatogr. A 1456 (2016) 10–18, https://doi.org/10.1016/j. chroma.2016.05.096.
- [34] M. Xiao, P. Li, Y. Lu, J. Cao, H. Yan, Development of a three-dimensional porous ionic liquid-chitosan-graphene oxide aerogel for efficient extraction and detection of polyhalogenated carbazoles in sediment samples, Talanta 271 (2024) 125711, https://doi.org/10.1016/j.talanta.2024.125711.
- [35] M.R. Afshar Mogaddam, S. Beiramzadeh, M. Nazari Koloujeh, A. Changizi Kecheklou, M.M. Daghi, M.A. Farajzadeh, M. Tuzen, Sorbent-based extraction procedures. Green Analytical Chemistry: Current Status and Future Perspectives in Sample Preparation, Elsevier, 2024, pp. 59–117, https://doi.org/10.1016/B978-0-443-16122-3.00011-1.
- [36] T. Chaipet, S. Maneeratanachot, N. Lehman, E. Kalkornsurapranee, W.C. Mak, P. Kanatharana, P. Thavarungkul, C. Thammakhet-Buranachai, Two-pot synthesis of polypyrrole-coated rubber foam for the extraction of carbendazim residue in orange juice, Microch. J. 207 (2024) 111712, https://doi.org/10.1016/j. microc.2024.111712.
- [37] R. Thati, B.S. Seetha, P. Alegete, M.K.R. Mudiam, Molecularly imprinted dispersive micro solid-phase extraction coupled with high-performance liquid chromatography for the determination of four aflatoxins in various foods, Food Chem. 433 (2024) 137342, https://doi.org/10.1016/j.foodchem.2023.137342.
- [38] F. Al-Hammashi, F. Momenbeik, Polycatechol coated cigarette filter as a sorbent for microextraction by packed sorbent of acidic non-steroidal anti-inflammatory drugs (NSAIDs) from wastewater samples, Microchem. J. 208 (2025) 112298, https://doi.org/10.1016/j.microc.2024.112298.
- [39] A. Talita María da Silva, L.Aparecida Fonseca Dinali, K.Bastos Borges, Microextraction by packed sorbent using core-shell molecularly imprinted polymer as adsorbent and capillary electrophoresis for determination of amlodipine enantiomers from human urine, Microchem. J. 205 (2024) 111372, https://doi. org/10.1016/j.microc.2024.111372.
- [40] L.A.F. Dinali, H.L. de Oliveira, L.S. Teixeira, W. de Souza Borges, K.B. Borges, Mesoporous molecularly imprinted polymer core@shell hybrid silica nanoparticles as adsorbent in microextraction by packed sorbent for multiresidue determination of pesticides in apple juice, Food Chem 345 (2021) 128745, https://doi.org/ 10.1016/j.foodchem.2020.128745.

- [41] European Commission, EU Pesticides Database, European Union Food Safety, https://food.ec.europa.eu/plants/pesticides/eu-pesticides-database_en, 2025. accessed July 17, 2025.
- [42] M.A.P.A. Santiago, J.P. dos Anjos, M.M. Nascimento, G.O. da Rocha, J.B. de Andrade, A miniaturized simple binary solvent liquid phase microextraction (BS-LPME) procedure for pesticides multiresidues determination in red and rose wines, Microchem. J. 167 (2021) 106306, https://doi.org/10.1016/j. microc.2021.106306.
- [43] W. Wojnowski, M. Tobiszewski, F. Pena-Pereira, E. Psillakis, AGREEprep Analytical greenness metric for sample preparation, TrAC Trends Anal. Chem. 149 (2022) 116553, https://doi.org/10.1016/j.trac.2022.116553.
- [44] N. Manousi, W. Wojnowski, J. Płotka-Wasylka, V. Samanidou, Blue applicability grade index (BAGI) and software: a new tool for the evaluation of method practicality, Green. Chem. 25 (2023) 7598–7604, https://doi.org/10.1039/ d3gc02347h.
- [45] T. Sun, Y. Fan, P. Fan, F. Geng, P. Chen, F. Zhao, Use of graphene coated with ZnO nanocomposites for microextraction in packed syringe of carbamate pesticides from juice samples, J. Sep. Sci. 42 (2019) 2131–2139, https://doi.org/10.1002/issr.201900257
- [46] N.G. Pereira dos Santos, D.A.V. Medina, F.M. Lanças, Microextraction by packed sorbent of N-nitrosamines from Losartan tablets using a high-throughput robot platform followed by liquid chromatography-tandem mass spectrometry, J. Sep. Sci. 46 (2023) 202300214, https://doi.org/10.1002/jssc.202300214.
- [47] M.M. Nascimento, J.P. dos Anjos, M.L. Nascimento, C.S. Assis Felix, G.O. da Rocha, J.B. de Andrade, Development of a green liquid-phase microextraction procedure using a customized device for the comprehensive determination of legacy and current pesticides in distinct types of wine samples, Talanta 266 (2024) 124914, https://doi.org/10.1016/j.talanta.2023.124914.
- [48] C. Dal Bosco, F. Mariani, A. Gentili, Hydrophobic eutectic solvent-based dispersive liquid-liquid microextraction applied to the analysis of pesticides in wine, Molecules 27 (2022) 27030908, https://doi.org/10.3390/molecules27030908.